Thermal versus mechanical unfolding of ubiquitin

ARTICLE *in* PROTEINS STRUCTURE FUNCTION AND BIOINFORMATICS · NOVEMBER 2006

Impact Factor: 2.63 · DOI: 10.1002/prot.21145 · Source: PubMed

2 AUTHORS, INCLUDING:

Simon Mitternacht
University of Bergen
20 PUBLICATIONS **384** CITATIONS

SEE PROFILE

PROTEINS: Structure, Function, and Bioinformatics 65:759–766 (2006)

Thermal Versus Mechanical Unfolding of Ubiquitin

Anders Irbäck* and Simon Mitternacht
Complex Systems Division, Department of Theoretical Physics, Lund University, Sölvegatan 14A, SE-223 62 Lund, Sweden

ABSTRACT **The authors studied the temperature-induced unfolding of ubiquitin by all-atom Monte Carlo simulations. The unfolding behavior is compared with that seen in previous simulations of the mechanical unfolding of this protein, based on the same model. In mechanical unfolding, secondary-structure elements were found to break in a quite well-defined order. In thermal unfolding, the authors saw somewhat larger event-to-event fluctuations, but the unfolding pathway was still far from random. Two long-lived secondary-structure elements could be identified in the simulations. These two elements have been found experimentally to be the thermally most stable ones. Interestingly, one of these long-lived elements, the first β-hairpin, was found to break early in the mechanical unfolding simulations. Their combined simulation results thus enable the authors to predict in detail important differences between the thermal and mechanical unfolding behaviors of ubiquitin. Proteins 2006;65: 759–766.** © 2006 Wiley-Liss, Inc.

Key words: protein folding; temperature-induced unfolding; force-induced unfolding; all-atom model; Monte Carlo simulation

INTRODUCTION

Ubiquitin is a 76-residue α/β protein, whose unfolding and refolding properties have been extensively studied experimentally. It was first thought that an intermediate state is populated during the folding of this protein.[1] More recent studies suggest, however, that ubiquitin folds in a two-state manner in the absence of stabilizing salt.[2,3]

In its native form, ubiquitin contains an α-helix packed against a five-stranded β-sheet (Fig. 1). The thermally most stable parts of the native structure seem to be the α-helix and the first (N-terminal) β-hairpin, which is part of the β-sheet. An NMR-based study of the temperature dependence of hydrogen bonds found that these secondary-structure elements are more resistant to temperature increases than the remaining three β-strands.[5] That the first β-hairpin is thermally more stable than the rest of the β-sheet has also been concluded from IR spectroscopy.[6] Interestingly, the α-helix and the first β-hairpin have been found to be relatively resistant to cold denaturation as well.[7]

There is evidence that the same two secondary-structure elements, the α-helix and the first β-hairpin, form early as ubiquitin folds to its native conformation. An extensive ϕ-value analysis, based on 27 mutations throughout the protein, found that both these structures are present in the transition state, but that the rest of the molecule remains largely unstructured at this stage of folding.[8] It has also been suggested, based on a ψ-value analysis, that two additional β-strands are present in the transition state.[9] The reason for these somewhat different conclusions has been discussed.[10,11]

In addition to studies of full-length ubiquitin, there have also been experiments on various excised fragments of the protein, including the first β-hairpin[12] (residues 1–17) and the α-helix[13] (residues 21–35). Both these peptides showed a tendency, although weak, to make nativelike structure, whereas the 36–76-residue fragment showed little or no such tendency.[13]

Together, the experiments strongly suggest that the α-helix and the first β-hairpin are relatively resistant to several different types of perturbations. Recently, however, we suggested, based on all-atom Monte Carlo (MC) simulations, that the situation is different in mechanical unfolding.[14] The mechanical unfolding of ubiquitin has been studied in several single-molecule experiments.[15–19] One of these studies investigated the unfolding behavior under a constant stretching force, using end-to-end linked polyubiquitin.[17] In this study, ubiquitin was seen to unfold in a two-state manner in most events, but several examples of unfolding through intermediate states were also observed. The difference in end-to-end distance between the native and typical intermediate states was consistent with what one would expect if the α-helix and the first β-hairpin survived whereas the rest of the β-sheet unfolded,[17] which would be in line with the above-mentioned findings at zero force. However, in the presence of a stretching force of $\geq$100 pN, the energy landscape is strongly tilted, and the unfolding behavior might very well be different from that at zero force. Important differences between mechanical and thermal unfolding have in fact been seen in simulations of other proteins, such as the I27 domain of titin.[20,21]

The results from our previous study of the mechanical unfolding of ubiquitin[14] are indeed different from the ex-

Grant sponsor: Swedish Research Council.

*Correspondence to: Anders Irbäck, Complex Systems Division, Department of Theoretical Physics, Lund University, Sölvegatan 14A, SE-223 62 Lund, Sweden. E-mail: anders@thep.lu.se

Received 18 January 2006; Revised 6 April 2006; Accepted 27 May 2006

Published online 5 September 2006 in Wiley InterScience (www.interscience.wiley.com). DOI: 10.1002/prot.21145

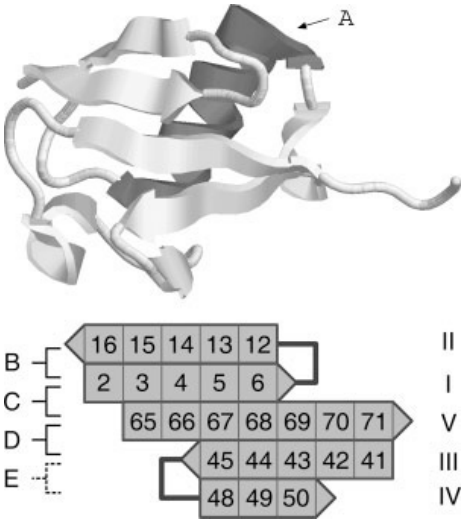

Fig. 1. Schematic illustrations of the native structure of ubiquitin with our labels for secondary-structure elements, A–E. (Top) A 3D model (Protein Data Bank code 1d3z, first model) drawn with RasMol.[4] (Bottom) The organization of the β-sheet. Residue numbers, strand labels (I–V) and two β-hairpin turns are indicated.

perimental results on the thermal unfolding of this protein. In particular, we found that the first β-hairpin broke early in the simulations, so that the typical unfolding intermediate contained the α-helix and the other three β-strands, but not the first β-hairpin. This behavior contrasts sharply with the observed stability of this β-hairpin in zero-force experiments. The mechanical unfolding experiments[17] monitored only the end-to-end distance. Our results for this quantity were in good agreement with the experimental results. Both one-step unfolding and unfolding through intermediate states occurred in our simulations, and properties such as the size of the unfolding step, the frequency of occurrence of intermediate states, and the position of the typical intermediate state were all found to be in reasonable agreement with the experimental data.

Here we perform an MC study of the thermal unfolding of ubiquitin, using the same model and methods as in our study of the force-induced unfolding of this protein.[14] In this way, we can directly compare thermal and force-induced unfolding. To ensure representative sampling, we generated a set of 800 thermal unfolding events for our analysis.

Computational studies of ubiquitin folding and unfolding at zero force have been reported by several groups. Perhaps the work most relevant to ours is an all-atom molecular dynamics study with explicit water,[22] which found that the native contacts between the β-strands I and V (see Fig. 1) as well as those in the first β-hairpin were lost early in thermal unfolding. These findings are not in perfect agreement with experimental data. However, the statistics were limited to two unfolding trajectories, and it might be worth noting that contacts in the first β-hairpin did not disappear completely but fluctuated with time. In addition to this all-atom molecular dynamics study, there have been studies using coarse-grained approaches,[23–25] threading algorithms,[26] and an MC design strategy.[27] The force-induced unfolding of ubiquitin has also been studied using both all-atom[14,15,28] and coarse-grained[29,30] models. Atomic-level simulations of force-induced unfolding have been reported for several other proteins as well, such as immunoglobulin and fibronectine type III domains of titin.[20,31–33]

MATERIALS AND METHODS

The model we use combines an atomistically detailed chain representation with a simplified force field, which was developed by folding studies of a set of well characterized peptides.[34,35] Both α-helical and β-sheet peptides were studied. In addition to peptide folding, this model has also been used to study peptide aggregation[36] and the force-induced unfolding of ubiquitin,[14] without changing any model parameters.

The model contains all atoms of the protein chain, including hydrogen atoms, but no explicit water molecules. It assumes fixed bond lengths, bond angles, and peptide torsion angles (180°), so that each amino acid only has the Ramachandran torsion angles ϕ, Ψ and a number of side-chain torsion angles as its degrees of freedom. The interaction potential

$$E = E_{\mathrm{loc}} + E_{\mathrm{ev}} + E_{\mathrm{hb}} + E_{\mathrm{hp}} \qquad (1)$$

is composed of four terms. The term E_{loc} is local in sequence and represents an electrostatic interaction between adjacent peptide units along the chain. The other three terms are nonlocal in sequence. The excluded volume term E_{ev} is a $1/r^{12}$ repulsion between pairs of atoms. E_{hb} represents two kinds of hydrogen bonds: backbone–backbone bonds and bonds between charged side chains and the backbone. The last term E_{hp} represents an effective hydrophobic attraction between nonpolar side chains. It is a simple pairwise additive potential based on the degree of contact between two nonpolar side chains. The precise form of the different interaction terms and the numerical values of all geometry parameters can be found elsewhere.[34,35]

The potential in Eq. (1) provides, despite its simplicity, a good description of the structure and folding thermodynamics of several peptides with different native geometries.[35] For ubiquitin, which is significantly larger than these peptides, it is unclear whether the native state corresponds to the global free-energy minimum of the model. In our thermal unfolding simulations, the temperature was set to 368 K, which is higher than, but close to, the melting temperature of ubiquitin (~90°C).[37] At this temperature, refolding should not be extremely rare, but it did not occur in our simulations. This indicates that the model underestimates the statistical weight of the native state, so that effectively the temperature is higher than 368 K in the simulations. The focus of the present study is not on the overall stability of the native

state but rather on the relative stability of different parts of the native structure, which is determined by the shape of the free energy in a small neighborhood of the native minimum. From our previous ubiquitin study,[14] it is known that the native state indeed is a pronounced local free-energy minimum of the model. Also, it was shown that the model reproduces key observations in the single-molecule constant-force experiments.[17]

Our simulations were carried out using the program package PROFASI,[38] which is a C++ implementation of this model. A model structure with a root-mean-square deviation (RMSD) of <0.5 Å from the NMR-derived native structure[39] was determined by simulated-annealing-based minimization. This optimized model structure served as the starting point for our simulations. The unfolding process was simulated using MC dynamics, with two move types. For the backbone, we used a semilocal method, Biased Gaussian Steps,[40] rather than single-variable updates, to avoid large unphysical deformations of the chain. This method turns up to eight adjacent angles simultaneously, with a bias toward local deformations of the chain. Side-chain angles, on the other hand, were updated one by one. The fractions of attempted backbone and side-chain moves were 25% and 75%, respectively. A total of 800 unfolding simulations were performed, each comprising 2.5×10^7 elementary MC steps.

A study of folding or unfolding kinetics based on MC dynamics must be interpreted with care, as discussed, for example, by Shakhnovich and coworkers.[41] Many detailed questions regarding the kinetics cannot be addressed this way; the short-time evolution of an individual MC trajectory may have very little to do with real dynamics. However, the sequence of major events will be dictated by the free-energy landscape rather than the precise choice of dynamics, provided that a "small step," detailed-balance-obeying algorithm is used. Here it is essential that the events are separated by many elementary MC steps, and that they are observed in an ensemble of trajectories. A comparison of MC and Brownian dynamics was made in a study of α-helical hairpins,[42] where the two methods were found to give the same folding pathway.

To delineate the unfolding process, we examine the order of breaking of four secondary-structure elements, A–D, which are indicated in Figure 1. The structure A is the α-helix, whereas B–D are three pairs of adjacent strands in the β-sheet. In our analysis of mechanical unfolding,[14] we also followed the fourth pair of adjacent strands in the five-stranded β-sheet, labeled E in Figure 1. The structure E is a small β-hairpin with one pair of properly hydrogen bonded amino acids, namely, 45 and 48, and one additional backbone hydrogen bond between amino acids 43 and 50. This structure, with residues that are close in sequence, broke and partly reappeared many times in the simulations, although complete restoration was very rare. As a result, the time of breaking becomes difficult to define for E. Therefore, and because of its small size, this structure is omitted from our analysis.

To what degree the structures A–D are present at a given stage in unfolding is determined by monitoring native backbone hydrogen bonds. A hydrogen bond is considered formed if the energy is lower than a cutoff.[35] The structures A–D contain a total of 20 backbone hydrogen bonds. The fraction of these 20 bonds that are present in a given conformation is denoted by n_{hb}.

The times at which the structures A–D break in the simulations show large event-to-event fluctuations (see Results); both the "waiting time" before unfolding starts and the actual unfolding time vary substantially from event to event. To filter these variations out of the analysis and focus on the order of events, we study the unfolding process as a function of some unfolding coordinate x rather than MC time.

To investigate the dependence of the individual hydrogen bonds on the unfolding coordinate x, we divide the x-axis into bins. For each unfolding event, we then compute the fraction of configurations in the different bins that contain a given hydrogen bond. In this way, we obtain an x-profile for each hydrogen bond and each event. Finally, we compute an average x-profile for each hydrogen bond, by averaging over all events. This procedure assigns equal weight to all the events, irrespective of the time spent in the different bins. In our study of mechanical unfolding,[14] we averaged over all data without first computing profiles for the individual events, which effectively means that the events were weighted by the time spent in the different bins. The definition adopted here is somewhat more robust. The change of definition alters the precise shape of the curves, but does not affect any of our previous conclusions regarding the mechanical unfolding simulations.

In the case of mechanical unfolding, the end-to-end distance r is an obvious choice for the unfolding coordinate x. For thermal unfolding, there are several conceivable choices of x, including the above-mentioned fraction of native hydrogen bonds, n_{hb}, the RMSD from the native state, and the fraction of native contacts. Below, we use n_{hb} as unfolding coordinate. A difference between this coordinate and the fraction of native contacts is that the former does not take into account contacts between the α-helix and the β-sheet. However, in our simulations, these two coordinates were strongly correlated and therefore essentially equivalent. The correlation coefficient was 0.96. The correlation between n_{hb} and the RMSD from the native state was slightly weaker, with a coefficient of -0.78. We found n_{hb} to be a more suitable choice than the RMSD when studying the order of breaking of the structures A–D. The separation between these structures was clearer in the profiles with n_{hb} as unfolding, or x, coordinate than in those with the RMSD as x coordinate.

In addition to this event-averaged analysis of the unfolding order of the structures A–D, we also perform an analysis of all individual events. Here we directly analyze the time of breaking of these structures, rather than using n_{hb}.

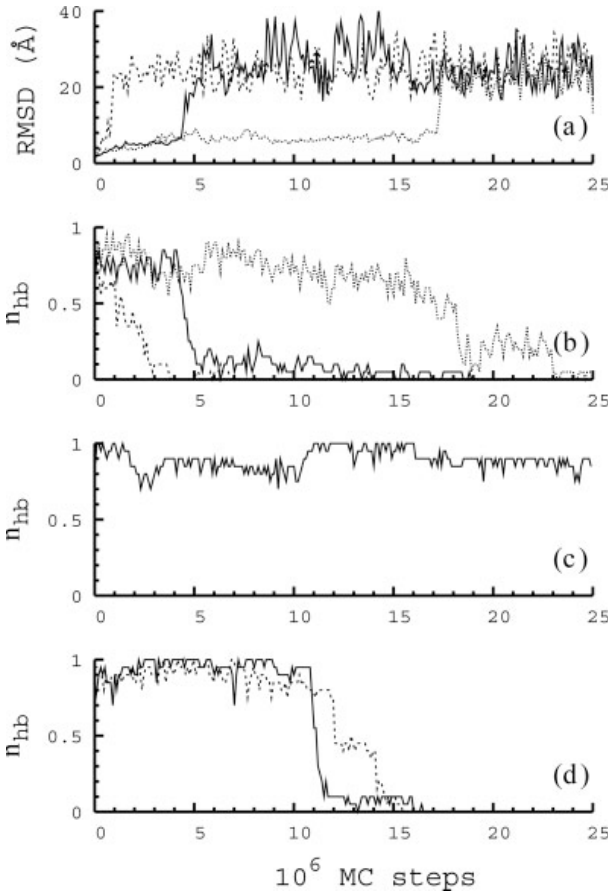

Fig. 2. MC evolution in representative runs with and without applied force. (**a**) RMSD from the native structure in three runs at 368 K and zero force. (**b**) The fraction of native backbone hydrogen bonds in the structures A–D, n_{hb}, in the same three runs. (**c**) n_{hb} in a control simulation at 288 K and zero force. (**d**) n_{hb} in two simulations of mechanical unfolding at 288 K and a force strength of 100 pN.

RESULTS

Using the model and methods described in Material and Methods, we performed 800 high-temperature simulations of ubiquitin at 368 K, all starting from the native structure but with different random number seeds. Figure 2(a,b) illustrates three representative runs, by showing the time evolution of the RMSD from the native structure (calculated over all nonhydrogen atoms) and the native hydrogen bond fraction n_{hb} (see Materials and Methods), respectively. The protein unfolded within the simulated MC time interval in virtually all runs, and often early on. However, many runs begin with a "waiting period," in which the protein molecule remains nativelike, typically with $n_{hb} \sim 0.7$ and an RMSD of $\sim$5 Å. This period, whose extent varies from run to run, is followed by rapid unfolding. The existence of a waiting period shows that the native state is a local free-energy minimum of the model at the temperature studied, although thermal fluctuations are relatively large, as can be seen from the RMSD and n_{hb} data.

Figure 2(c) shows a control simulation at low temperature, 288 K. At this temperature, the molecule remained nativelike throughout the simulated time interval, with n_{hb} typically above 0.8, which is higher than in the waiting phase at 368 K.

Finally, Figure 2(d) shows two runs from our study of force-induced unfolding,[14] for a force of 100 pN and a temperature of 288 K. In one of these runs, unfolding is seen to occur in a single step. The other trajectory halts for a while at $n_{hb} \sim 0.4$ before unfolding continues. The plateau at $n_{hb} \sim 0.4$ signals a significantly populated intermediate state. Comparing our temperature- and force-induced events, we find that the unfolding process tends to be somewhat less abrupt in the thermal case, although event-to-event variations are large. Another difference is that we do not find any evidence of well-defined reoccurring intermediate states in thermal unfolding.

To get a more detailed picture of the unfolding process, we now turn to the order of breaking of the four secondary-structure elements labeled A–D in Figure 1, which is investigated by measuring native backbone hydrogen bonds (see Materials and Methods). Figure 3 illustrates how the presence of these hydrogen bonds varies with the degree of unfolding in our simulations of thermal as well as mechanical unfolding. The unfolding coordinate is $1-n_{hb}$ in the thermal case and the end-to-end distance r in the mechanical case. In the mechanical unfolding simulations [see Fig. 3(b)], it is immediately clear that the structures A–D tend to break in a certain order, namely, CBDA. The points at which the different structures break are less well defined and less separated in the thermal case [see Fig. 3(a)]. Nevertheless, it is evident that the unfolding order is not entirely random in the thermal unfolding simulations either. Specifically, it can be seen that C again has a tendency to break first. However, in the thermal case, C is followed by D rather than B. The order in which the remaining two structures A and B break is harder to decide; they are both partially present for essentially all values of the unfolding parameter $1 - n_{hb}$. Inevitably, all structures disappear as $1 - n_{hb}$ approaches one.

Figure 3 provides an idea of what the preferred unfolding orders are in the thermal and mechanical unfolding simulations, respectively. To quantify how strong these statistical preferences are, it is necessary to refine the analysis of Figure 3, which deals solely with averages over all events and hence does not tell how large event-to-event fluctuations are. An extended event-based analysis was carried out for the mechanical unfolding simulations.[14] Here we basically follow the same procedure, although some details are different. For each individual event, we determine an unfolding path (a permutation of ABCD), by directly analyzing the time of breaking of the structures A–D. A structure is deemed intact, at a given time, if one-half or more of its native backbone hydrogen bonds are present, and the time of breaking is defined as the last point in time after which the structure is never found intact. With these criteria, we

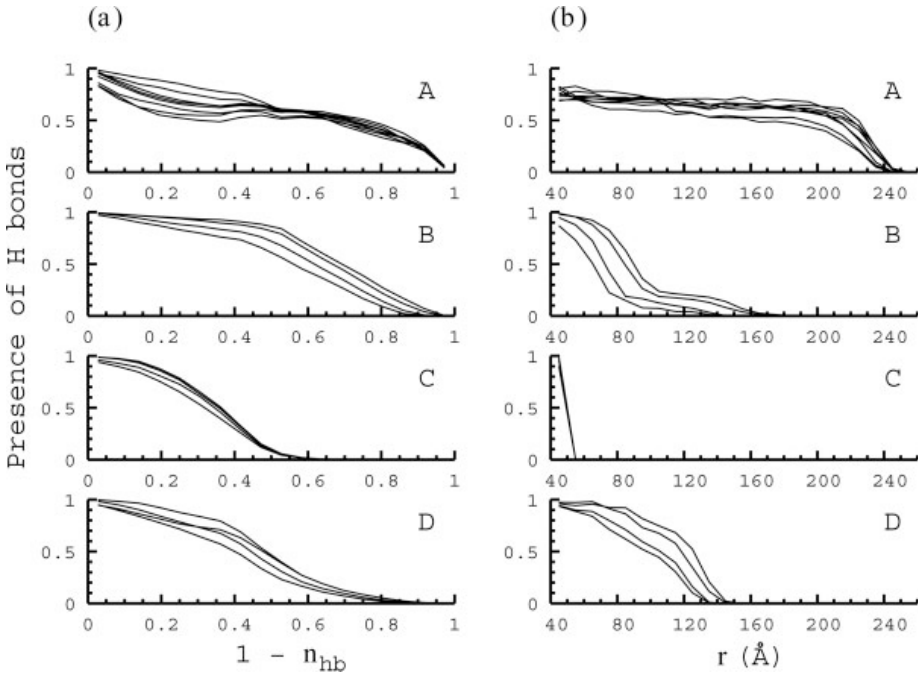

Fig. 3. Presence of native backbone hydrogen bonds during unfolding, for the structures A–D (see Fig. 1). Each curve represents one hydrogen bond, and is an average over all runs. The structure A has eight native backbone hydrogen bonds, whereas the other three structures have four bonds each. (**a**) Temperature-induced unfolding at 368 K (and zero force), with $1-n_{hb}$ as unfolding coordinate, where n_{hb} is the fraction of native backbone hydrogen bonds in A–D. (**b**) Force-induced unfolding at 288 K and 100 pN, with the end-to-end distance r as unfolding coordinate.

find that 66% of our mechanical unfolding events follow the path CBDA (at 100 pN and 288 K). Another 21% of the events have the order of B and D apparently interchanged, the path being CDBA. In these events, B does unfold before D but then partially reforms after D is gone. This behavior can be regarded as a minor variation of the path CBDA, which means that 87% of the events follow the same basic pathway. The partial refolding of B in the apparent CDBA events is responsible for the tail of the curves for B in Figure 3(b).

Repeating the same analysis for our thermal unfolding simulations leads to a different picture. As expected from Figure 3(a), there is no similarly dominant path in this case; the most common path is CDBA with a frequency of occurrence of 44%. Nevertheless, some definite trends can be seen in the thermal unfolding data as well. In particular, there is a clear tendency for C and D to be the first structures to break. Among the six possible pairs of the structures A–D, this pair breaks first in 76% of the events. The event-based analysis thus confirms that both C and D tend to break before B, as suggested by Figure 3(a). Compared with the preferred mechanical unfolding path, this result implies that the order of B and D is interchanged in a majority of the thermal unfolding events.

Especially for thermal unfolding, where event-to-event fluctuations are larger, it is instructive to directly compare the times of breaking of the structures A–D by means of scatter plots. Figure 4 shows t_i, t_j scatter plots, where t_i and t_j are the times of breaking of structures i and j, for all the six possible pairs of the structures A–D. In all six cases, there is a clear tendency for one of the structures to break before the other. Particularly clear are the relations $t_C < t_A$, $t_C < t_B$, and $t_D < t_A$, which are fulfilled in 796, 786, and 747 events, respectively (out of 800). These strong statistical preferences clearly reveal that the unfolding order is less random than what one might expect from the event-averaged results shown in Figure 3(a). For the remaining three pairs of structures, we find that $t_C < t_D$, $t_D < t_B$, and $t_B < t_A$ hold in 644, 640, and 633 of the events, respectively.

DISCUSSION

Using an all-atom model with a simplified interaction potential, we have examined the thermal unfolding of ubiquitin. In particular, we analyzed the unfolding order of four major secondary-structure elements, labeled A–D, based on a set of 800 unfolding events. This analysis showed that there was no single statistically dominant unfolding pathway, but the unfolding order of A–D was nevertheless far from random. In particular, we found that the structures A and B, the α-helix and the first β-hairpin, typically survived longer than C and D in the

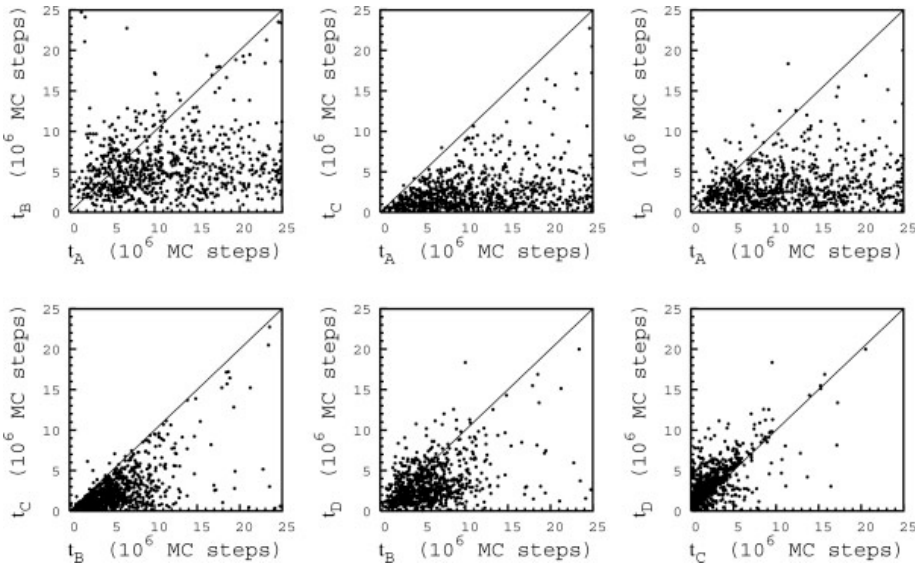

Fig. 4. t_i, t_j scatter plots, where t_i and t_j denote the times of breaking of structures i and j, for all the six possible pairs of the structures A–D. Each data point represents one unfolding simulation.

simulations. Among six possible pairs of structures, the pair A and B was the last to break in ~75% of the events. Experimentally, these two structures have been found to be the thermally most stable ones.[5,6] Our results support this conclusion.

There are both similarities and differences between our thermal and mechanical[14] unfolding results for this protein. One difference is that the unfolding behavior was more deterministic in the mechanical case, where a statistically preferred unfolding order could be identified (CBDA). Another difference is that while B typically was the second structure to break in those simulations, B along with A are the structures that tend to survive longest in the thermal unfolding simulations. A similarity between the two sets of unfolding events is that the structure C tends to break first in both cases.

The results from the mechanical unfolding simulations can be compared with data from single-molecule constant-force experiments.[17] However, these experiments monitored only the end-to-end distance, and therefore do not provide any detailed information about the unfolding pathway. There is, by contrast, experimental information available about the thermal stability of different parts of the ubiquitin structure,[5,6] and our thermal unfolding results are, as mentioned above, consistent with these experiments. This agreement in the thermal case provides support for our calculated but experimentally unverified unfolding order for the mechanical case, since the model and methods were the same in both our studies.

The fact that we observe different pathways in thermal and mechanical unfolding is not surprising, because our study of the mechanical unfolding was, like the experiments,[17] carried out for stretching forces of 100 pN or more. Such a large force shifts the energy balance between the native and typical intermediate states by as much as ~100 pN × 7 nm ~100 kcal/mol. Hence, there is no reason to expect the unfolding behavior to be the same as at zero force.

Nevertheless, it is interesting to try to identify and compare the major factors dictating the thermal and mechanical unfolding behaviors. It is well known that pulling geometry, in relation with native topology, is a major determinant of a protein's mechanical resistance.[15,43] Pulling geometry and topology also explain why the ubiquitin elements C and B break early in our mechanical unfolding events. That C breaks first is inevitable, because the stretching forces act on C and cannot be sensed by the other parts until C is broken. The native state is mechanically resistant because C is pulled longitudinally, so that several hydrogen bonds must break simultaneously. Once C is gone, the β-hairpin B is free to unzip, one bond at a time. Unzipping requires less force than separation by longitudinal pulling, which makes B likely to break quickly when no longer protected by C.

As mentioned earlier, differences between thermal and mechanical unfolding have been seen in previous simulations of, for example, the I27 domain of titin.[20,21] For this β-sandwich protein, it was found that the breaking of contacts between its two β-sheets was an early event when stretching the protein, but occurred late in thermal unfolding. On the other hand, it was found that the same three β-strands are unfolded last in both thermal and mechanical unfolding. For ubiquitin, our results suggest that the most long-lived β-strands are different in thermal and mechanical unfolding, respectively.

In pulling the ends of a protein some elements of the structure are exposed to force while others are not. In thermal unfolding, there is no external force acting

selectively on certain parts of the protein. Instead, unfolding is driven by thermal fluctuations. As a result, intrinsic stabilities should become more important. The parts of ubiquitin that are thermally most stable, A and B, both consist of connected stretches of residues along the sequence. The local character makes it possible for these structures to reform spontaneously. Experimentally, it has been found that the excised peptides A and B both have a tendency to make nativelike structure,[12,13] which shows that these structures possess an intrinsic stability. The structure element that tends to break first in the simulations, C, is, on the other hand, the only parallel β-sheet structure in the native state, and might have a relatively low intrinsic stability due to a different hydrogen bond geometry and other factors. These observations show that differences in intrinsic stability might, indeed, partly explain the behavior seen in our thermal unfolding simulations. However, there are also other factors that should be important. In particular, it is worth noting that the structure C has a key role in the native topology; it connects the two ends of the chain and occupies a central position in the β-sheet. As a result, C is likely to play an important protecting role in thermal unfolding as well, and not only in the mechanical case where the external forces acted on this particular structure.

Finally, we wish to stress that our studies of the both thermal and the mechanical unfolding of ubiquitin were performed using the same model, without adjusting any parameters. There are peptides that this model, developed by studies of peptide folding, fails to fold.[35] Nevertheless, it is encouraging that this model, with its relatively simple potential, is able to capture relevant features seen in thermal as well as mechanical unfolding experiments on ubiquitin. To what extent the applicability of the model can be extended to a wider spectrum of sequences, by refinement of the potential, remains to be seen.

ACKNOWLEDGMENTS

The authors thank Sandipan Mohanty for discussions and computational assistance.

REFERENCES

1. Khorasanizadeh S, Peters ID, Roder H. Evidence for a three-state model of protein folding from kinetic analysis of ubiquitin variants with altered core residues. Nat Struct Biol 1996;3:193–205.
2. Krantz BA, Sosnick TR. Distinguishing between two-state and three-state models for ubiquitin folding. Biochemistry 2000;39: 11696–11701.
3. Went HM, Benitez-Cardoza CG, Jackson SE. Is an intermediate state populated on the folding pathway of ubiquitin? FEBS Lett 2004;567:333–338.
4. Sayle RA, Milner-White EJ. RasMol: biomolecular graphics for all. Trends Biochem Sci 1995;20:374–376.
5. Cordier F, Grzesiek S. Temperature-dependence of protein hydrogen bond properties as studied by high-resolution NMR. J Mol Biol 2002;317:739–752.
6. Chung HS, Khalil M, Smith AW, Ganim Z, Tokmakoff A. Conformational changes during the nanosecond-to-millisecond unfolding of ubiquitin. Proc Natl Acad Sci USA 2005;102:612–617.
7. Babu CR, Hilser VJ, Wand AJ. Direct access to the cooperative substructure of proteins and the protein ensemble via cold denaturation. Nat Struct Mol Biol 2004;11:352–357.
8. Went HM, Jackson SE. Ubiquitin folds through a highly polarized transition state. Protein Eng Des Sel 2005;18:229–237.
9. Krantz BA, Dothager RS, Sosnick TR. Discerning the structure and energy of multiple transition states in protein folding using ψ-analysis. J Mol Biol 2004;337:463-475 (erratum, J Mol Biol 2005; 347:1103).
10. Fersht AR. Φ value versus ψ analysis. Proc Natl Acad Sci USA 2004;101:17327–17328.
11. Sosnick TR, Dothager RS, Krantz BA. Differences in the folding transition state of ubiquitin indicated by ϕ and ψ analyses. Proc Natl Acad Sci USA 2004;101:17377–17382.
12. Zerella R, Evans PA, Ionides JMC, Packman LC, Trotter BW, Mackay JP, Williams DH. Autonomous folding of a peptide corresponding to the β-hairpin from ubiquitin. Protein Sci 1999;8: 1320–1331.
13. Jourdan M, Searle MS. Cooperative assembly of a nativelike ubiquitin structure through peptide fragment complexation: energetics of peptide association and folding. Biochemistry 2000;39: 12355–12364.
14. Irbäck A, Mitternacht S, Mohanty S. Dissecting the mechanical unfolding of ubiquitin. Proc Natl Acad Sci USA 2005;102:13427–13432.
15. Carrion-Vazquez M, Li H, Lu H, Marszalek PE, Oberhauser AF, Fernandez JM. The mechanical stability of ubiquitin is linkage dependent. Nat Struct Biol 2003;10:738–743.
16. Fernandez JM, Li H. Force-clamp spectroscopy monitors the folding trajectory monitors the folding trajectory of a single protein. Science 2004;303:1674–1678.
17. Schlierf M, Li H, Fernandez JM. The unfolding kinetics of ubiquitin captured with single-molecule force-clamp techniques. Proc Natl Acad Sci USA 2004;101:7299–7304.
18. Sarkar A, Robertson RB, Fernandez JM. Simultaneous atomic force microscope and fluorescence measurements of protein unfolding using a calibrated evanescent wave. Proc Natl Acad Sci USA 2004;101:12882–12886.
19. Chyan CL, Lin FC, Peng H, Yuan JM, Chang CH, Lin SH, Yang G. Reversible mechanical unfolding of single ubiquitin molecules. Biophys J 2004;87:3995–4006.
20. Paci E, Karplus M. Unfolding proteins by external forces and temperature: the importance of topology and energetics. Proc Natl Acad Sci USA 2000;97:6521–6526.
21. Cieplak M, Sulkowska J. Thermal unfolding of proteins. J Chem Phys 2005;123:194908.
22. Alonso DOV, Daggett V. Molecular dynamics simulations of hydrophobic collapse of ubiquitin. Protein Sci 1998;7:860–874.
23. Sorenson JM, Head-Gordon T. Toward minimalist models of larger proteins: a ubiquitin-like protein. Proteins 2002;46:368–379.
24. Sosnick TR, Berry RS, Colubri A, Fernández A. Distinguishing foldable proteins from nonfolders: when and how do they differ? Proteins 2002;49:15–23.
25. Zhang J, Qin M, Wang W. Multiple folding mechanisms of protein ubiquitin. Proteins 2005;59:565–579.
26. Gilis D, Rooman M. Identification and ab initio simulations of early folding units in proteins. Proteins 2001;42:164–176.
27. Michnick SW, Shakhnovich E. A strategy for detecting the conservation of folding-nucleus residues in protein superfamilies. Fold Des 1998;3:239–251.
28. Li PC, Makarov DE. Simulation of the mechanical unfolding of ubiquitin: probing different unfolding reaction coordinates by changing the pulling geometry. J Chem Phys 2004;121:4826–4832.
29. Kirmizialtin S, Huang L, Makarov DE. Topography of the free-energy landscape probed via mechanical unfolding of proteins. J Chem Phys 2005;122:234915.
30. Szymczak P, Cieplak M. Stretching of proteins in a force-clamp. J Phys: Condens Matter 2006;18:L21–L28.
31. Lu H, Schulten K. Steered molecular dynamics simulations of force-induced protein domain unfolding. Proteins 1999;35:453–463.
32. Lu H, Schulten K. The key event in force-induced unfolding of titin's immunoglobulin domains. Biophys J 2000;79:51–65.
33. Fowler SB, Best RB, Herrera JLT, Rutherford TJ, Steward A, Paci E, Karplus M, Clarke J. Mechanical unfolding of a titin Ig

domain: structure of unfolding intermediate revealed by combining AFM, molecular dynamics simulations, NMR and protein engineering. J Mol Biol 2002;322:841–849.
34. Irbäck A, Samuelsson B, Sjunnesson F, Wallin S. Thermodynamics of α- and β-structure formation in proteins. Biophys J 2003; 85:1466–1473.
35. Irbäck A, Mohanty S. Folding thermodynamics of peptides. Biophys J 2005;88:1560–1569.
36. Favrin G, Irbäck A, Mohanty S. Oligomerization of amyloid $A\beta_{16-22}$ peptides using hydrogen bonds and hydrophobicity forces. Biophys J 2004;87:3657–3664 (erratum, Biophys J 2005;89:754).
37. Wintrode PL, Makhatadze GI, Privalov PL. Thermodynamics of ubiquitin unfolding. Proteins 1994;18:246–253.
38. Irbäck A, Mohanty S. PROFASI: a Monte Carlo simulation package for protein folding and aggregation. J Comp Chem 2006; 27:1548–1555.
39. Cornilescu G, Marquardt JL, Ottiger M, Bax A. Validation of protein structure from anisotropic carbonyl chemical shifts in a dilute crystalline phase. J Am Chem Soc 1998;120:6836–6837.
40. Favrin G, Irbäck A, Sjunnesson F. Monte Carlo update for chain molecules: biased Gaussian steps in torsional space. J Chem Phys 2001;114:8154–8158.
41. Shimada J, Kussell EL, Shakhnovich EI. The folding thermodynamics and kinetics of crambin using an all-atom Monte Carlo simulation. J Mol Biol 2001;308:79–95.
42. Rey A, Skolnick J. Comparison of lattice Monte Carlo dynamics and Brownian dynamics folding pathways of α-helical hairpins. Chem Phys 1991;158:199–219.
43. Brockwell DJ, Paci E, Zinober RC, Beddard GS, Olmsted PD, Smith DA, Perham RN, Radford SE. Pulling geometry defines the mechanical resistance of a β-sheet protein. Nat Struct Biol 2003;10:731–737.